

The Pennsylvania State University

The Graduate School

College of Engineering

**CFD ANALYSIS OF DISPERSION OF CO₂ IN
OCCUPIED SPACE: EFFECT OF SENSOR POSITION**

A Thesis in

Architectural Engineering

by

Gen Pei

© 2018 Gen Pei

Submitted in Partial Fulfillment

of the Requirements

for the Degree of

Master of Science

August 2018

The thesis of Gen Pei was reviewed and approved* by the following

Donghyun Rim

Assistant Professor of Architectural Engineering

Thesis Advisor

William Bahnfleth

Professor of Architectural Engineering

Gregory Pavlak

Assistant Professor of Architectural Engineering

M. Kevin Parfitt

Professor of Architectural Engineering

Head of the Department of Architectural Engineering

*Signatures are on file in the Graduate School.

ABSTRACT

Demand-controlled ventilation (DCV) becomes more attractive to building system designers due to its potential to save energy while maintaining acceptable indoor air quality (IAQ). One of the most widely used DCV systems is based on the measurement of carbon dioxide (CO₂) concentration. In a CO₂-based DCV system, the supply airflow rate varies according to the signals from CO₂ sensors. However, limited information is available for the relationships between building environmental factors and the CO₂ dispersion in rooms as well as the performance of sensors positioned at various locations. This paper presents a numerically based study focusing on the effect of sensor position in rooms that are ventilated with CO₂-based DCV systems. A total of eight realistic scenarios were examined using experimentally validated Computational Fluid dynamic (CFD) models. The parametric analysis results revealed the impacts of three major parameters: 1) ventilation strategy (mixing vs. displacement), 2) air change rate, and 3) number of occupants on the CO₂ distribution and sensor performance. The results show that the CO₂ transport and the sensor readings notably vary with the ventilation strategy, air change rate and number of occupants. The CO₂ sensors placed at the exhaust show good performance for a DCV system with mixing ventilation while showing less accuracy with displacement ventilation. The results also suggest that sensors situated at wall at the breathing height (e.g., 1.2 m) can improve the measurement accuracy in displacement ventilation system compared to sensors located at the exhaust. The results indicate that the performance of the sensors placed on the office desk varies significantly with indoor airflow conditions and a careful prediction of the performance should be conducted before using them.

TABLE OF CONTENTS

LIST OF TABLES	v
LIST OF FIGURES	vi
1. Introduction	1
2. Methods	4
2.1 <i>Validation of CFD model</i>	4
2.1.1 <i>Experimental set-up</i>	4
2.1.2 <i>Description of CFD model: Geometry</i>	6
2.1.3 <i>Description of CFD model: Mesh generation</i>	6
2.1.4 <i>Description of CFD model: Numerical model</i>	7
2.1.5 <i>Description of CFD model: Boundary conditions</i>	8
2.1.6 <i>Validation process</i>	8
2.2 <i>Parametric study</i>	11
2.3 <i>Evaluation of CO₂ sensor performance</i>	13
3. Results and discussion	15
3.1 <i>CO₂ concentration distribution</i>	15
3.2 <i>Performance of CO₂ sensors placed at exhaust</i>	18
3.3 <i>Performance of CO₂ sensors placed at the breathing height and on the desk</i>	20
4. Conclusion	24
REFERENCES	27

LIST OF TABLES

Table 1. Technical data of the IAQ sensors	6
Table 2. Convective and radiative percentages of total sensible heat gain	8
Table 3. Simulated cases for the parametric analysis.....	11
Table 4. CO ₂ concentrations at exhaust and in the breathing zone (DV: displacement ventilation; MV: mixing ventilation; BZ: breathing zone)	20
Table 5. CO ₂ concentrations at exhaust, in the breathing zone and at six sampling points (DV: displacement ventilation; MV: mixing ventilation; BZ: breathing zone).....	23

LIST OF FIGURES

Figure 1. (a) Experiment set-up and sensors location; (b) manikin and CO ₂ emission tube.	5
Figure 2. Details of the computational grid.	7
Figure 3. CFD validation results: temperature (a) and CO ₂ concentration (b) at monitoring locations.	9
Figure 4. Diffuser arrangements in rooms with (a) displacement ventilation system; (b) mixing ventilation system.	12
Figure 5. Occupant arrangements in rooms with (a) 1 occupant; (b) 5 occupants.	12
Figure 6. Schematic diagram for (a) locations of sampling points; (b) breathing zone.	13
Figure 7. Distributions of steady-state CO ₂ concentration on the vertical sectional planes with five occupant.	16
Figure 8. Distributions of steady-state CO ₂ concentration on the horizontal sectional planes at the height of 0.3, 1.2 and 2.4 m with five occupant.	17
Figure 9. Profiles of transient CO ₂ concentration at exhaust and within the breathing zone with five occupants. Note that the horizontal scale is half in the graphs for ACH of 5 h ⁻¹ of those for ACH of 2.5 h ⁻¹	19
Figure 10. Comparisons between the steady-state CO ₂ concentrations at exhaust (Ex) and at sampling points S1-S6 to the average CO ₂ concentration in the breathing zone in the cases with five occupants.	21
Figure 11. Comparisons between the steady-state CO ₂ concentrations at exhaust (Ex) and at sampling points S1-S6 to the average CO ₂ concentration in the breathing zone in the cases with one occupant.	22

1. Introduction

In an occupied space, it is necessary to reduce the indoor pollutant concentrations by introducing adequate quantity of fresh air. Insufficient ventilation in an occupied room likely causes the increased health symptoms in occupants such as asthma and sick building syndrome (Daisey et al. 2003). However, increase of the ventilation as a single method to reduce the indoor pollutant concentration does not seem to be an energy saving strategy. A significant fraction of the space conditioning energy is used for providing the thermally conditioned outdoor air (Sherman and Matson 1997; Emmerich and Persily 1998). As a result, the demand-controlled ventilation (DCV) becomes more attractive to building system designers as it provides possibilities for energy conservation while maintaining the acceptable indoor air quality (IAQ).

DCV is the control strategy to vary the outdoor airflow provided to the occupied space based on the number of occupants or ventilation requirements of the space (ANSI/ASHRAE standard 62.1 2013). Several previous studies evaluated the performance of the DCV systems in different types of occupied space and found that a well-designed DCV system is able to achieve energy saving without compromising IAQ (Kusuda T 1976; Nielsen et al. 2010; Budaiwi and Al-Homoud 2001; Faulkner et al. 1996; Schibuola et al. 2016; Shan et al. 2012; Fisk and Almeida 1998). For instance, Fisk and Almeida (1998) reviewed the case studies of DCV system applied to various types of building and found that in appropriate applications, it produced significant energy savings with a payback period typically of a few years. Budaiwi and Al-Homoud (2001) used the theoretical models to examine the effect of different ventilation strategies on IAQ and cooling energy consumption for a single-zone enclosure. Results showed that when the strategy that varies ventilation based on occupancay was employed, a more than 50 % energy saving was achieved while maintaining the pollutant concentration below the recommended level. Schibuola

et al. (2016) analyzed the performance of the DCV system in a university library based on the measured data from the supervisory system and pointed out the DCV system allowed a 21% reduction of the amount of conditioned air, consequently achieved a 33% total primary energy saving in the monitored year.

One of the most widely used DCV systems is based on the measurement of carbon dioxide (CO₂) concentration (Fisk and Almeida 1998; Krarti et al. 2004; Nassif et al. 2005; Sun et al. 2011). In buildings, the occupants are normally the main CO₂ emission source. The indoor CO₂ concentration has been shown a reliable indicator of occupational exposure to the bioeffluents from humans (ASTM D6245-12 2012). In addition, CO₂ can be used as a tracer gas to evaluate the ventilation in buildings when the indoor CO₂ concentration exceeds the outdoor level (Persily 1997). Therefore, the indoor CO₂ concentrations are often monitored in buildings as a surrogate of ventilation rate and to evaluate the IAQ (Daisey et al. 2003; Lee and Chang 1999). Several standards have defined the allowable level for the indoor CO₂ concentration to maintain the acceptable IAQ. ANSI/ASHRAE Standard 62.1 (2013) states that maintaining a CO₂ concentration in a space no greater than about 700 ppm above outdoor air levels will indicate that a majority of occupants will be satisfied with respect to human bioeffluents. ASTM Standard D6245 (2012) suggests maintaining CO₂ concentrations within 650 ppm above outdoors should maintain body odor at an acceptable level.

Considering the contaminant concentration in the breathing zone normally can better reflects the occupational exposure, in a CO₂-based DCV system, the requirement of ventilation can be estimated based on the monitored breathing zone CO₂ concentration. However, the inappropriate CO₂ sensor arrangement (e.g., sensor density and location) may cause the inaccurate measurement. Previous studies have investigated the spatial distributions of CO₂ in occupied

spaces (Stymne et al. 1991; Mundt 1994; Mahyuddin and Awbi 2010; Mahyuddin and Awbi 2012a; Bulińska et al. 2014). The experiments conducted by Stymne et al. (1991) and Mundt (1994) revealed the vertical gradient of CO₂ concentration in rooms with displacement ventilation. Mahyuddin and Awbi (2010) examined the CO₂ dispersion in a test chamber and found significant vertical and horizontal variation in CO₂ concentration under mixing ventilation condition with low air flow rate. Bulińska et al. (2014) performed experimentally validated numerical simulations to predict the spread of CO₂ in a naturally ventilated bedroom, and reported non-uniform CO₂ distribution in the vicinity of occupants, window and radiator. Furthermore, Mahyuddin and Awbi (2012a) performed an extensive literature review and noted that most researchers and building designers prefer to place only one sensor at representative position to measure the CO₂ concentration in a room. Hence, to improve the performance of the DCV system, it is important to investigate the association between the sensor positioning and sensor performance in predicting the breathing zone CO₂ concentration.

However, the majority of previous investigations focus more on the measurement of average CO₂ concentration in the whole room. Limited researches examined the sampling strategy for the measurement of breathing zone concentration. Furthermore, the relationships between several building operating factors (e.g., ventilation strategy, air change rate and source strength) and the CO₂ measurement are still unclear.

Based on this background, two primary objectives of present study are as follows:

- 1) Examine the impacts of ventilation strategy, air change rate, and number of occupants on the spatial distribution of CO₂ in an occupied space.

2) Evaluate the effect of sensor position on the measurement of the breathing zone CO₂ concentration under different operating conditions of DCV systems.

2. Methods

In recent years, Computational Fluid Dynamics (CFD) has been widely employed as a powerful tool to simulate the airflow pattern and gaseous pollutants dispersion in an indoor environment (Bulińska et al. 2014; Mahyuddin and Awbi 2012b; Rim and Novoselac 2008; Ning et al. 2016; Zhuang et al. 2014). In present study, an experimentally validated CFD model was built to simulate a typical office and investigate the dispersion pattern of CO₂ generated by occupants under various conditions. This section presents the description of the validation process, applied CFD model and the parametric analysis.

2.1 Validation of CFD model

In a numerically based study, the numerical model should be carefully verified and validated to assure its accuracy before applying it to further study. Based on the recommendations regarding CFD validation process provided by Chen and Srebric (2002), this study conducted experimental investigations on the temperature and CO₂ concentration distributions in a full-scale environmental chamber and the measured data was used to validate the CFD model. Furthermore, for each CFD simulation, the mass and energy balances in the simulation domain were validated.

2.1.1 Experimental set-up

Full-scale experimental measurements were conducted in a 4.27 m × 4.27 m × 3 m (length × width × height) environmental chamber set up like a typical one-occupant office. Figure 1a presents the experimental set-up. A total of 415 W heat load was generated by indoor heat sources including one thermal manikin (91 W), one computer (108 W), one monitor (26 W) and

two lights (95 W for each). The cool air was supplied at flow rate of $0.0385 \text{ m}^3/\text{s}$ using a low momentum displacement diffuser ($1.215 \times 0.615 \text{ m}$) at the floor level. The supply air temperature was conditioned to $18 \text{ }^\circ\text{C}$. Room air was exhausted through four round outlets at the ceiling level. CO_2 was continuously released at the flow rate of $0.026 \text{ m}^3/\text{h}$ through a tube in the vicinity of the nose of manikin (see Figure 1b) to simply simulate the CO_2 emission due to breathing. This CO_2 emission rate was about 1.5 times higher than normally found average CO_2 generation rate in an office environment, and corresponds to about 2 MET (metabolic equivalent of task) in males (Persily and Jonge, 2017). The higher release rate was used due to equipment considerations, but was not considered problematic as it was within a reasonable range and present study focused on the difference between the monitored values. The measured initial CO_2 concentration in the chamber and in the supply air were 472 ppm.

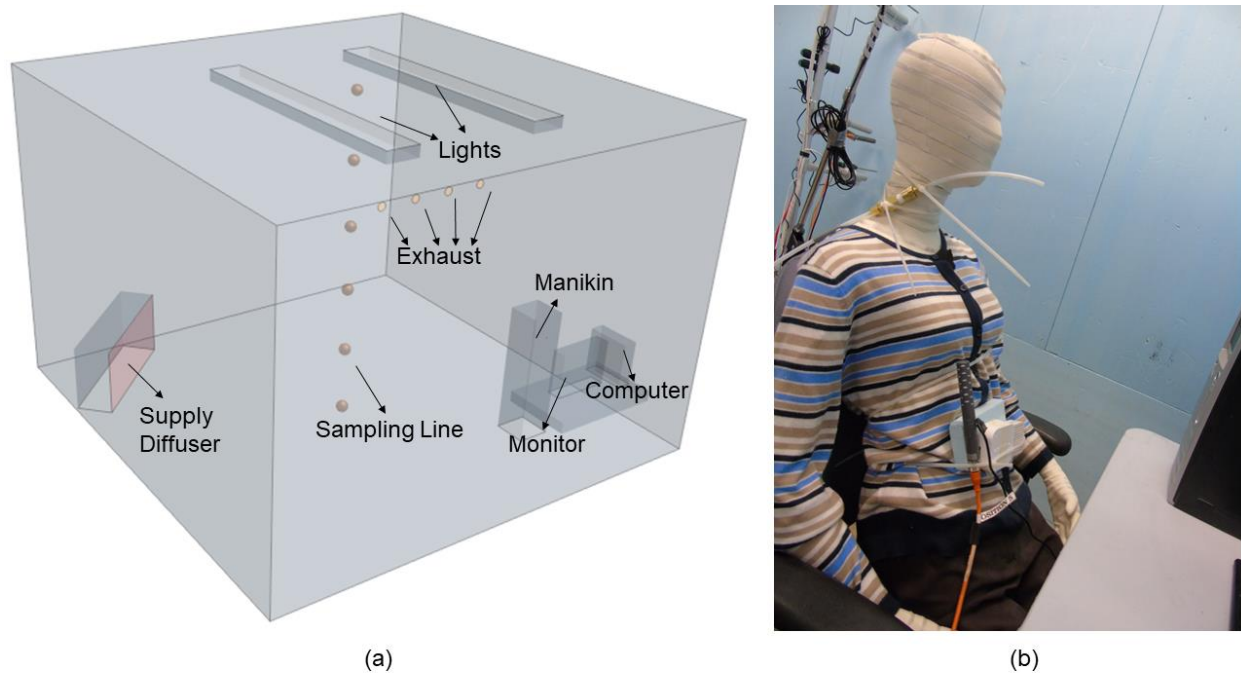


Figure 1. (a) Experiment set-up and sensors location; (b) manikin and CO_2 emission tube.

Vertical distributions of temperature and CO₂ concentration were measured at the center of the chamber (Figure 1a). Along this monitoring line, eight temperature sensors were placed at heights of 0.1, 0.3, 0.6, 1.1, 1.4, 1.7, 2.2, 2.6 m; and six CO₂ sensors were placed at heights of 0.3, 0.6, 1.1, 1.7, 2.2, 2.6 m. Table 1 summarizes the measurement ranges and accuracies of the sensors used in the experiments.

Table 1. Technical data of the IAQ sensors

Parameter	Accuracy	Range
CO ₂ sensor	±25 ppm ± 3% of reading	400-2000 ppm
Temperature sensor	±0.1°C	-20° to 70°C

2.1.2 Description of CFD model: Geometry

A three-dimensional geometry model was established based on the dimensions and set-up of the experimental chamber shown in Figure 1. The only difference is that the shape of the thermal manikin was simplified to a rectangular solid. Previous studies found that the simplified manikin geometry only affected the airflow in the vicinity of manikin, and was sufficient to simulate the global airflow (Topp et al. 2002; Deevy and Gobeau 2006). Since the present study investigated the overall airflow and CO₂ dispersion in the space, the simplified manikin geometry was employed.

2.1.3 Description of CFD model: Mesh generation

A computational grid was generated to discretize the geometry model using the polyhedral mesh due to its potential to save computational resources while providing good calculation accuracy (Peric and Ferguson 2012). The meshes were refined in the proximity of the heat sources (i.e., manikin, computer, monitor and lights), the air inlet and outlet, and the CO₂ inlet to more

accurately predict the heat and mass transfers in the simulation domain, as shown in Figure 2. The total number of the grid cells was equal to 169,285 for the simulation domain.

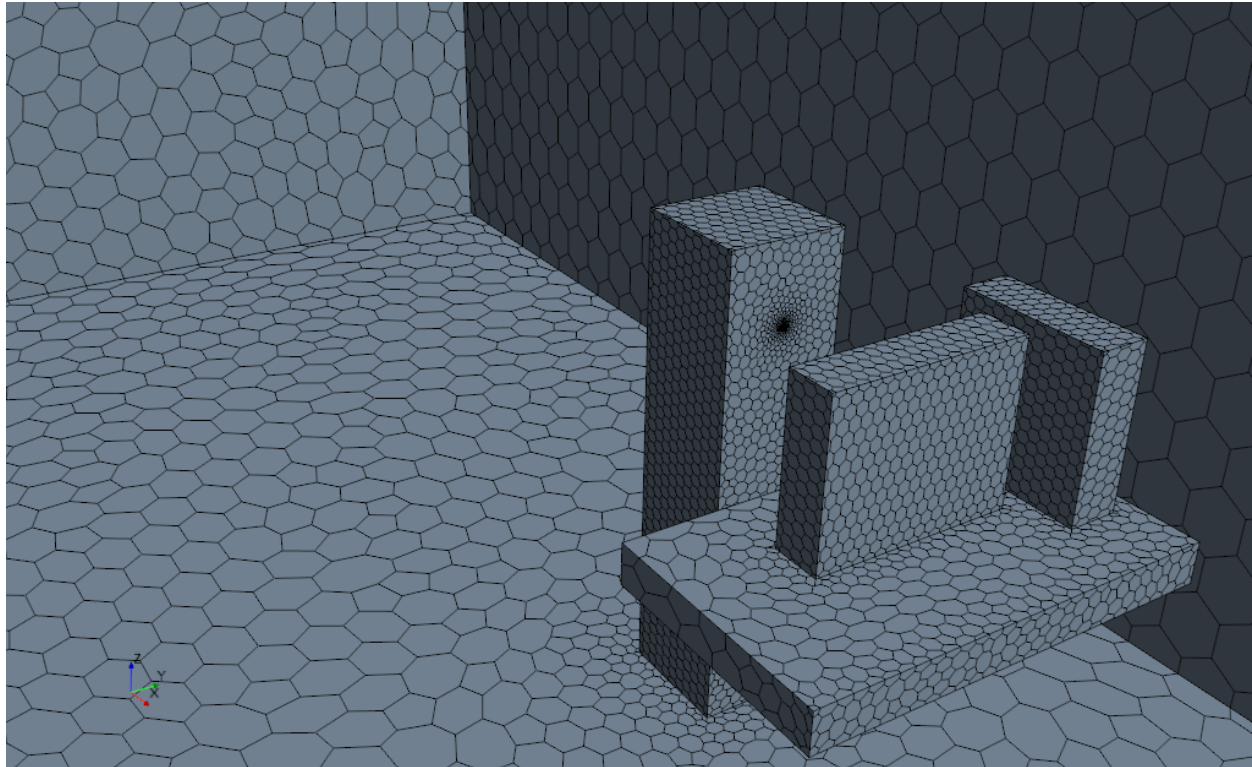


Figure 2. Details of the computational grid.

2.1.4 Description of CFD model: Numerical model

A commercial CFD software Star-CCM+ (2012) was used to compute the airflow and CO₂ transport in the space. The Reynolds Averaged Navier-Stokes (RANS) equations were employed with the two-equation Shear Stress Transport (SST) $k-\omega$ turbulence model. The SST $k-\omega$ turbulence model combines the advantages of both $k-\epsilon$ and $k-\omega$ models and shows good performance in predicting stratified indoor airflow associated with thermal plumes (Menter 1994; Argyropoulos and Markatos 2015; Gilani et al. 2016). Unsteady simulations were performed for a two hour period with a one second time step.

2.1.5 Description of CFD model: Boundary conditions

The boundary conditions applied in the CFD model were based on the experimental parameters, including the inlet air velocity and temperature, CO₂ emission rate, initial CO₂ concentration and the heat gain from indoor heat sources. Note that for simulations, the heat gain was divided into convective and radiative portions with recommended ratios in ASHRAE Handbook chapter 29 (2013). The total, radiative and convective heat loads for each indoor heat source are listed in Table 2. The radiative heat loads were distributed to the surrounding wall surfaces.

Table 2. Convective and radiative percentages of total sensible heat gain

Heat Source	Total Heat Gain (W)	Radiative		Convective	
		%	W	%	W
Occupant	91	58	52.78	42	38.22
Monitor	26	40	10.40	60	15.60
Computer	108	10	10.80	90	97.20
Light	95	67	63.65	33	31.35

2.1.6 Validation process

Figure 3 presents the comparisons between the simulated and measured temperature and CO₂ concentration vertical profiles at the center of the room. As shown in Figure 3a, it is observed that the temperature increases with height due to the fundamental principle of the displacement ventilation, which is in agreement with the previous study conducted by Mundt (1990). For the comparison, although the simulated temperatures do not perfectly agree with the measurements and a maximum discrepancy of 0.76 °C exists, the simulated temperature profile shows the similar trend with the measured data. Figure 3b illustrates the stratification of the CO₂ concentration in the displacement ventilated room which agrees with the previous researches (Stymne et al. 1991; Mundt 1994). Relatively large discrepancies of roughly 70 ppm and 90 ppm are observed near the floor likely due to the simplified geometry model of the thermal manikin,

which does not affect the overall CO₂ distribution in the space. When the height > 0.6 m, all the discrepancies between the simulated and measured concentrations are within the uncertainty of the CO₂ sensor. In addition, it is observed that the CO₂ distribution patterns obtained from simulation and measurement are similar. Considering it is challenging to simulate the stratified airflow pattern with displacement ventilation, the comparison results in Figure 3 suggest although the simulation and measurement results do not match perfectly, the CFD model can predict the general pattern of the thermal stratification and CO₂ transport in the room with acceptable accuracy, and it can be used for further numerical study.

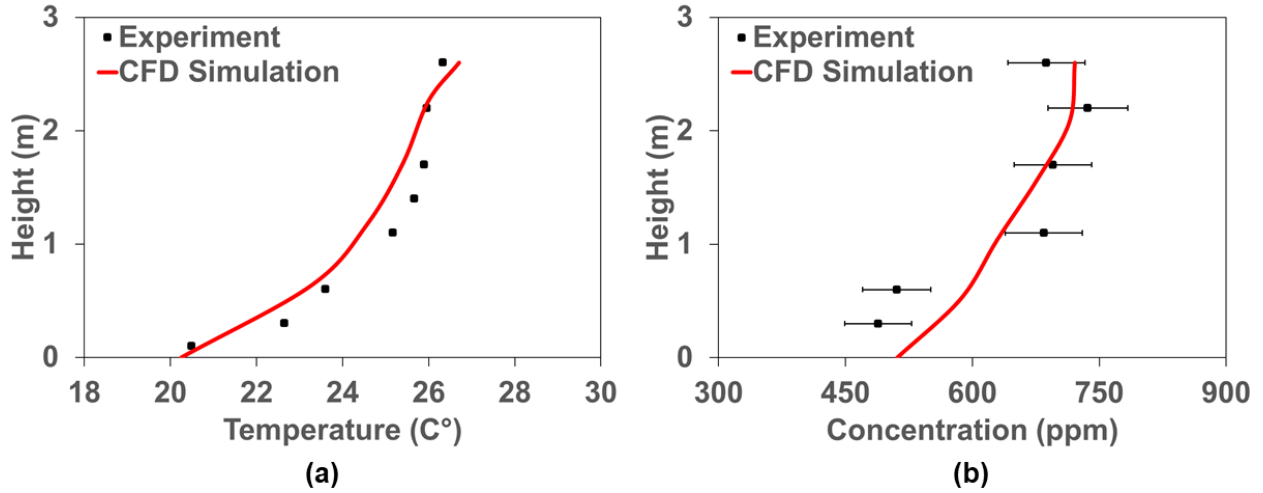


Figure 3. CFD validation results: temperature (a) and CO₂ concentration (b) at monitoring locations.

Furthermore, for each simulation, the mass and energy balances were validated. The difference between inlet and outlet flow rates was lower than 0.02%. The discrepancy between the simulated exhaust CO₂ concentration and theoretically calculated value from Eq. (1) was smaller than 1.3%.

$$C(t) = \frac{E}{Q} \times (1 - e^{-\lambda t}) \times 1000000 + C_s \quad (1)$$

where $C(t)$ = exhaust CO₂ concentration (ppm)

E = CO₂ generation rate (m³/s)

Q = air volumetric flow rate (m³/s)

λ = air change rate (h⁻¹)

C_s = supply CO₂ concentration (ppm)

t = solution time (h)

For the energy balance, the difference between the total heat generation and removal was lower than 0.01%. The discrepancy between the simulated exhaust air temperature and theoretically calculated value from Eq. (2) was within 0.3%. These results further demonstrate the accuracy of the CFD simulations.

$$q = \rho \times Q \times C_p \times (T_e - T_s) \quad (2)$$

where q = total heat load (W)

ρ = air density (kg/m³)

Q = air volumetric flow rate (m³/s)

C_p = air specific heat (J/(kg·K))

T_e = air temperature at the room exhaust (K)

T_s = supply air temperature (K)

2.2 Parametric study

The experimentally validated CFD model was further used for the parametric study. Previous study showed the ventilation scheme and pollutant source arrangement can influence the contaminant transport in the space. Rim and Novoselac (2008) examined the dispersion of SF₆ in two different airflow regimes: mixing flow and buoyant flow, and found that the temporal and spatial variations of SF₆ concentration were larger with buoyant flow. The study conducted by Rim and Novoselac (2009) illustrated the distribution of gaseous pollutant in the vicinity of occupants was more uniform with mixing flow than that with stratified flow. Maldonado and Woods (1983) summarized that three main factors can affect the indoor contaminant distributions: the location and strength of the pollutant source, the internal air movements as well as the type and location of the exchange with outdoor air. Therefore, the present study investigated the impacts of three major parameters including 1) ventilation strategy (mixing vs. displacement), 2) air change rate and 3) number of occupants on the CO₂ dispersion and measurement in the room, and a total of 8 cases were tested as listed in Table 3.

Table 3. Simulated cases for the parametric analysis

Case	Ventilation Strategy	Supply Air Temperature(°C)	Air Change Rate(h ⁻¹)	Supply Air Velocity (m/s)	Number of Occupants
1	Displacement	18	2.5	0.05	1
2			2.5	0.05	5
3			5	0.1	1
4			5	0.1	5
5	Mixing	16	2.5	1	1
6			2.5	1	5
7			5	2	1
8			5	2	5

Figure 4 shows the diffuser configurations and positions in the simulations with displacement ventilation and mixing ventilation. The operating factors of displacement ventilation system were

based on the experiments. For the mixing ventilation, the outdoor air was supplied through a $0.196\text{ m} \times 0.196\text{ m}$ large momentum diffuser at the ceiling level. The supply air temperature was maintained at $16\text{ }^{\circ}\text{C}$. For both cases, two air change rates, i.e. 2.5 h^{-1} and 5 h^{-1} were taken into account. A total of 4 cases with different ventilation schemes were built. For each case, two scenarios with different number of occupants (i.e., 1 occupant and 5 occupants) were simulated. Figure 5 presents the arrangements of the occupants.

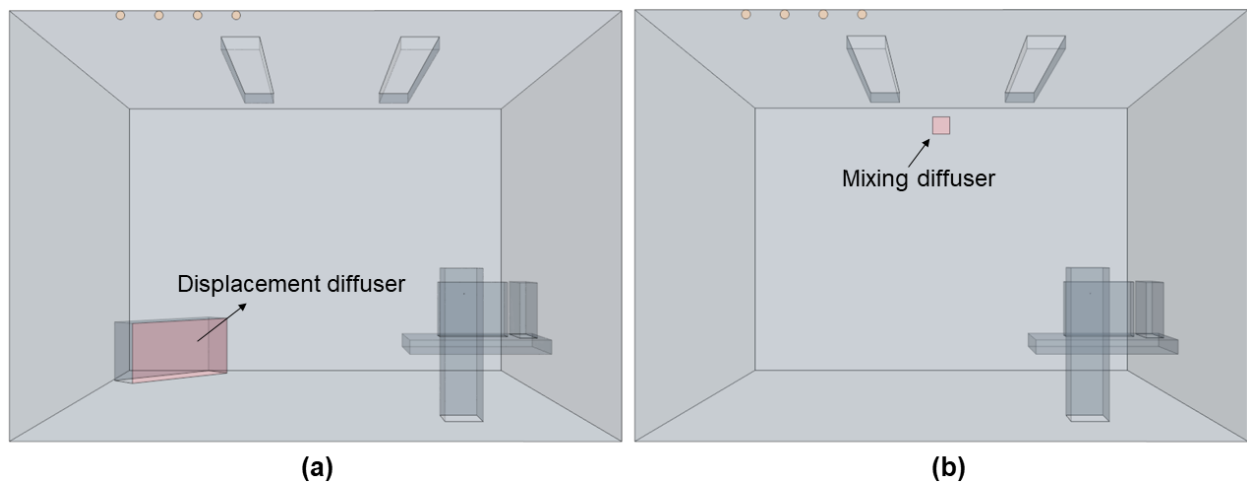


Figure 4. Diffuser arrangements in rooms with (a) displacement ventilation system; (b) mixing ventilation system.

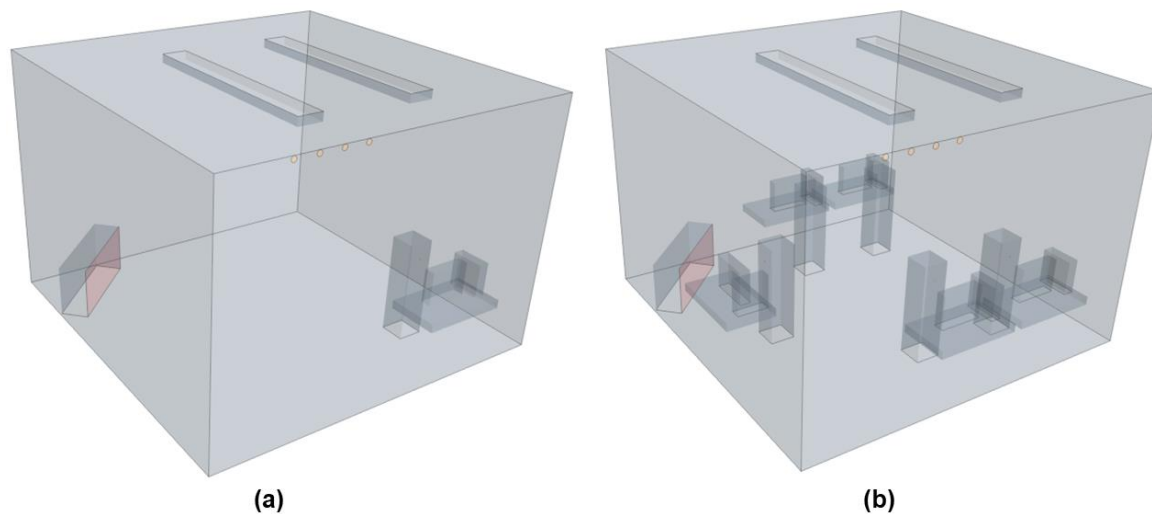


Figure 5. Occupant arrangements in rooms with (a) 1 occupant; (b) 5 occupants.

In summary, a total of 8 test cases were simulated to examine the effects of the ventilation strategy, air change rate and the number of occupants.

2.3 Evaluation of CO₂ sensor performance

For all 8 cases, the CO₂ was continuously injected from occupants and the space achieved steady-state condition after a period of time. The spatial distributions of CO₂ concentration in the room were measured.

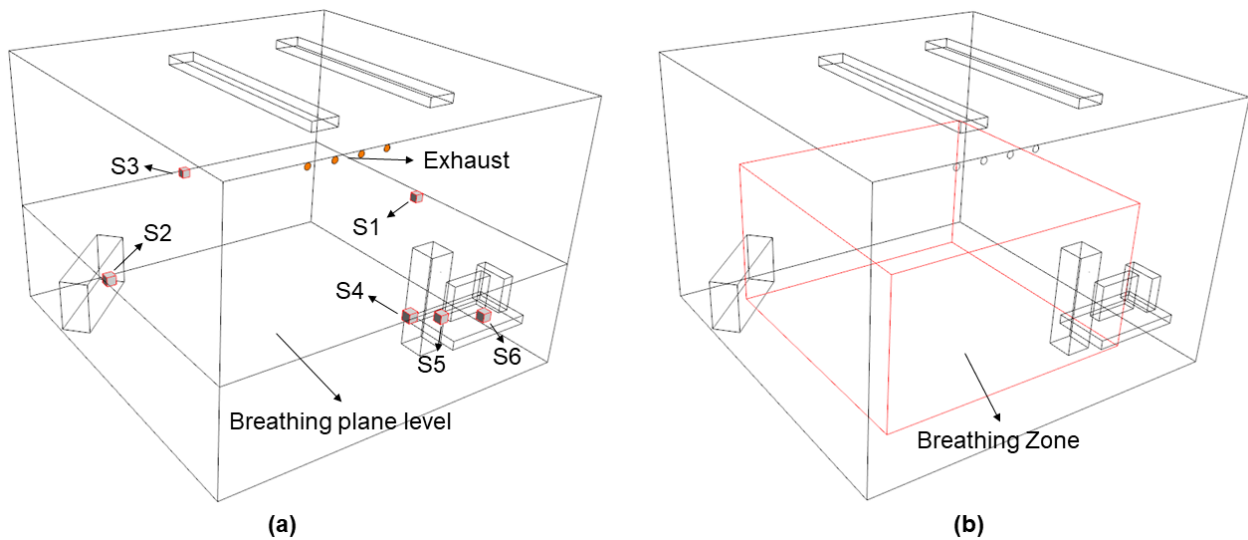


Figure 6. Schematic diagram for (a) locations of sampling points; (b) breathing zone.

To evaluate the effect of the sensor position on the measurement of the breathing zone CO₂ concentration, the local concentrations were monitored at various sampling locations (see Figure 6a) including:

- 1) At exhaust, to evaluate the performance of sensors placed at the return duct.

2) At four sampling points (S1-S4) situated at four sidewalls at the height of 1.2 m, to represent the sensors placed at wall at the normally considered breathing height for a sedentary occupant, i.e. the height ranging from 1.0 to 1.2 m above the floor.

3) At two sampling points (S5-S6) placed on the desk beside and behind the monitor, to test the performance of sensors situated on the typical office desk.

Along with the local CO₂ concentration measurements, the average CO₂ concentration within the breathing zone, i.e. the space between planes 7.55 and 180 cm above the floor and further than 60 cm from the walls (ANSI/ASHRAE standard 62.1 2013) (see Figure 6b), was calculated. The comparisons between the breathing zone concentration with the concentrations at different sampling locations provided the insight into the selection of the sensor position for the measurement of the breathing zone CO₂ concentration.

To quantitatively evaluate the performance of CO₂ sensors, two tolerance levels around the breathing zone concentration were defined based on the recommendation of Bulińska et al. (2014):

1) Tolerance level I. $\pm 10\%$ accuracy of the average CO₂ concentration in the breathing zone.

This tolerance uncertainty is allowed by ASTM E741-11 (2011) for representing the average gas concentration in the zone.

2) Tolerance level II. The accuracy of CO₂ sensors used in measurements, i.e. $\pm 25 \text{ ppm} \pm 3\%$ of measured value in present study. Considering the background CO₂ concentration in present study is 472 ppm, the tolerance level II is stricter than level I.

3. Results and discussion

The study results are organized into three sections. The first section presents the CO₂ distribution patterns under different conditions. The second section focuses on the performance of the CO₂ sensors placed at exhaust. The last section elaborates on the performance of the sensors situated at other sampling positions

3.1 CO₂ concentration distribution

Figure 7 shows the contours of the steady-state CO₂ concentration distribution along the vertical planes in four cases with five occupants. As shown in figure 7a, with displacement ventilation and ACH of 2.5 h⁻¹, the notable stratification of CO₂ concentration is created. The difference between the concentrations at floor and ceiling levels is about 900 ppm. This significant vertical variation is caused by the characteristics of the displacement ventilation, which forms the buoyancy-driven thermal plumes around the heat sources that transport the contaminants to the upper region. When the ACH is 5 h⁻¹ (see figure 7c), the stratification still exists but with less gradient. The difference between the concentrations at floor and ceiling levels is about 500 ppm. This is due to the larger ventilation rate that leads to a smaller concentration difference between inlet and outlet.

However, with mixing ventilation, as shown in figure 7b and 7d, no noticeable stratification of CO₂ concentration occurs in the space, and the concentration distributions are more uniform than those with displacement ventilation. The reason is in the mixing ventilation system, the supply air exits the inlet at a high velocity and induces room air to achieve a mixing airflow condition. When the ACH is 2.5 h⁻¹ (see figure 7b), although the high concentration flow still occurs in the vicinity of occupants, in the rest of the region, the variation is lower than 100 ppm. This variation

is due to the relatively small ACH which is not sufficient to mix the air well. When the ACH increases to 5 h^{-1} (see figure 7d), little spatial variation is observed, suggesting the well-mixed condition is achieved.

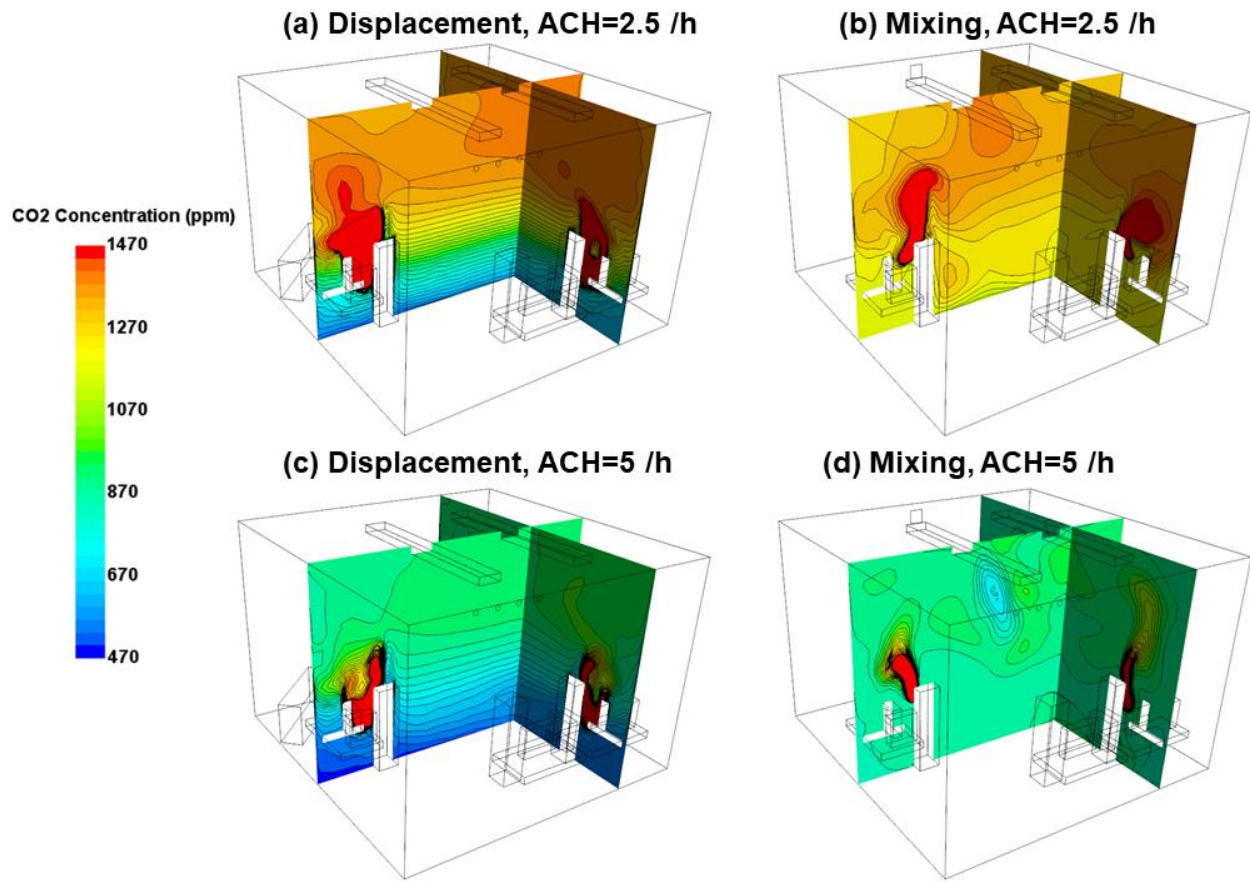


Figure 7. Distributions of steady-state CO_2 concentration on the vertical sectional planes with five occupant.

To get insight into the horizontal distribution, the CO_2 concentration profiles along horizontal planes at the height of 0.3, 1.2 and 2.4 m are presented in Figure 8. As shown in Figure 8a and 8c, with displacement ventilation system, it is apparent the CO_2 concentration varies with height. When the ACH is 2.5 h^{-1} (see figure 8a), the average concentrations along planes at 0.3, 1.2 and 2.4 m are 600, 1000 and 1300 ppm respectively. When ACH is 5 h^{-1} (see figure 8c), the

respective average concentrations are 400, 700 and 1000 ppm. However, for each horizontal plane, the concentration distribution is nearly uniform except for the region in the proximity of the emission sources. With mixing ventilation, when the ACH is 5 h^{-1} (see figure 8d), both the horizontal and vertical CO_2 distributions are quite homogeneous. With ACH of 2.5 h^{-1} (see Figure 8b), only roughly 100 ppm vertical variation is observed.

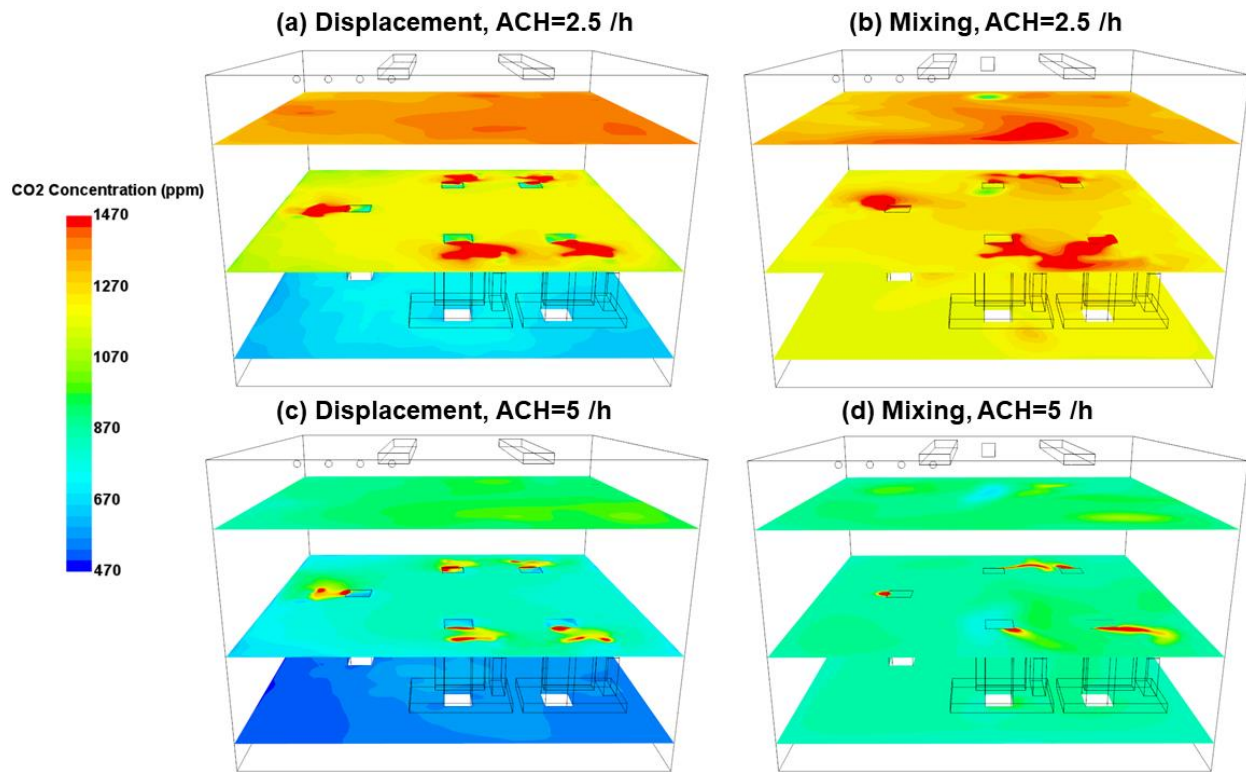


Figure 8. Distributions of steady-state CO_2 concentration on the horizontal sectional planes at the height of 0.3, 1.2 and 2.4 m with five occupant.

Taken together, the displacement ventilation can cause the stratification of the CO_2 concentration, whereas mixing ventilation creates more uniform CO_2 distribution. The results from the simulations with one occupant also illustrate the same pattern, but the pattern is less noticeable because of a lower CO_2 emission.

3.2 Performance of CO₂ sensors placed at exhaust

To evaluate the possibility of the CO₂ sensors situated at the return duct to predict the breathing zone concentration, Figure 9 compares the transient CO₂ concentration profiles at exhaust and within the breathing zone for cases with five occupants. As shown in Figure 9a, with displacement ventilation and ACH of 2.5 h⁻¹, the concentrations increase with time and get stabilized after about 90 mins. When the steady-state is achieved, the CO₂ concentration at exhaust is notably larger than that in the breathing zone and the difference is 228 ppm. This considerable difference is caused by the concentration stratification in the displacement ventilated room. When the ACH increases to 5 h⁻¹ (see figure 9c), it only requires about 45 mins to achieve the steady-state. It is still apparent that the exhaust CO₂ concentration exceeds the breathing zone concentration, but the difference is reduced to 99 ppm due to a less vertical concentration variation. In both these two scenarios, the differences exceed the tolerance level I (see Table 4), indicating with displacement ventilation, the measured value from sensor placed at return duct cannot accurately represent the breathing zone CO₂ concentration.

For the cases with mixing ventilation, the differences between the CO₂ concentrations at exhaust and in the breathing zone are notably reduced than those with displacement ventilation (see figure 9b and 9d). This is due to a more uniform CO₂ distribution created by the mixing airflow. It is also observed that the difference decreases with the larger ACH, which is 53 ppm with ACH of 2.5 h⁻¹ and is 21 ppm with 5 h⁻¹. For both these two cases, the differences are within the tolerance level II (see Table 4), suggesting the sensors placed at exhaust can accurately predict the breathing zone concentration and the discrepancies lay in the uncertain of the sensor used in the experiments.

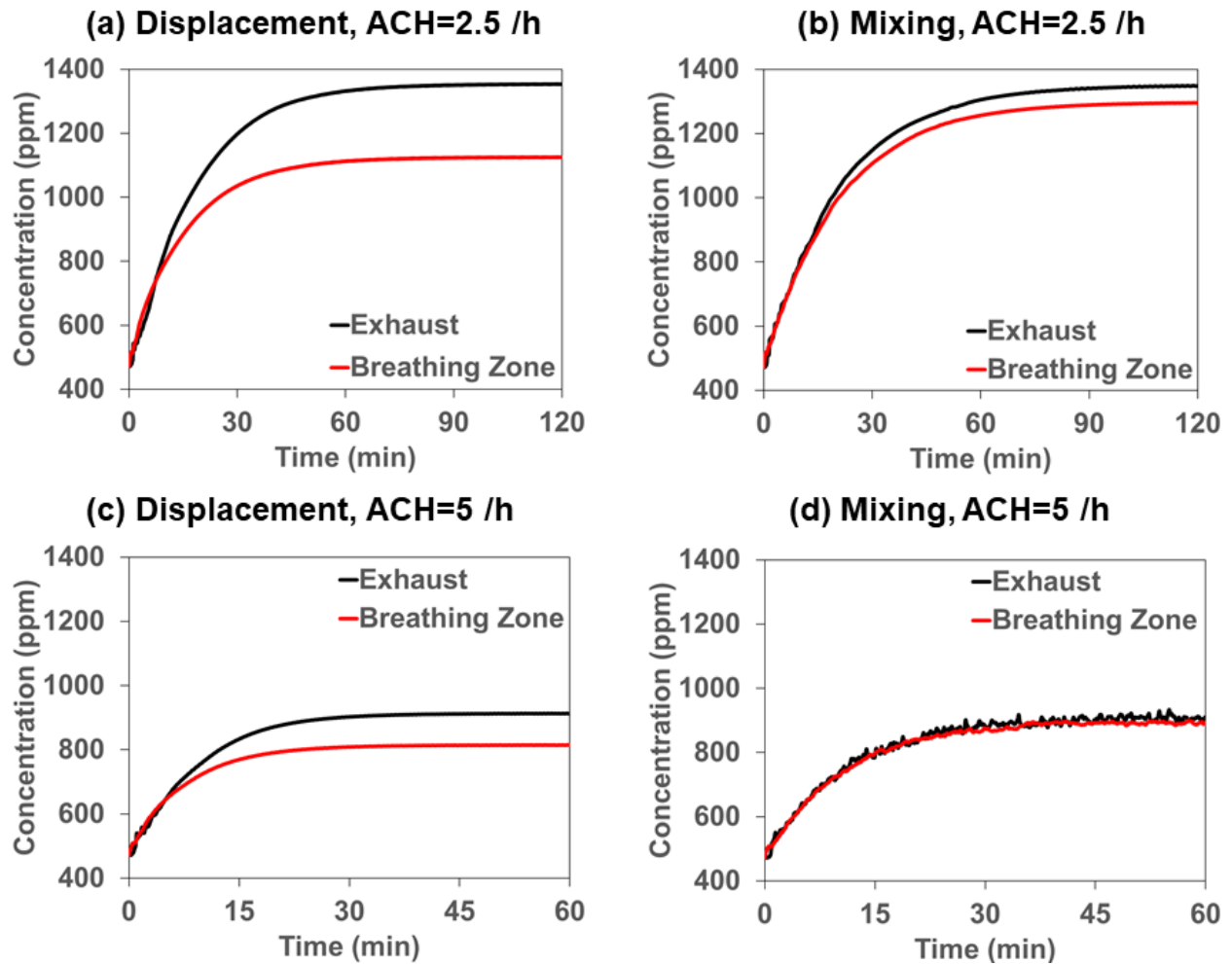


Figure 9. Profiles of transient CO₂ concentration at exhaust and within the breathing zone with five occupants. Note that the horizontal scale is half in the graphs for ACH of 5 h⁻¹ of those for ACH of 2.5 h⁻¹.

Generally, these results suggest that only in the mixing ventilated room, the CO₂ sensors placed at exhaust can accurately predict the breathing zone concentration, whereas the sensors can cause large discrepancies with displacement ventilation. The results from cases with one occupants show the similar trend. However, because of a quite lower CO₂ emission, even the largest discrepancy occurring in the case with displacement ventilation and ACH of 2.5 h⁻¹ is only 50 ppm and within the tolerance level I (see Table 4), indicating with low occupancy, the inaccuracy of the sensor may be acceptable even with displacement ventilation. Table 4

summarises the steady-state CO₂ concentrations at exhaust and in the breathing zone and compares the differences between these two concentrations to the tolerance levels.

Table 4. CO₂ concentrations at exhaust and in the breathing zone (DV: displacement ventilation; MV: mixing ventilation; BZ: breathing zone)

Ventilation	ACH (h ⁻¹)	Occupant number	Steady-state CO ₂ concentration (ppm)			Accuracy (ppm)	
			BZ	Exhaust	Difference	Tolerance level I	Tolerance level II
DV	2.5	1	599	648	50	60	43
DV	5		521	560	39	52	41
MV	2.5		615	647	31	62	43
MV	5		536	552	16	54	41
DV	2.5	5	1125	1353	228	113	59
DV	5		814	913	99	81	49
MV	2.5		1296	1349	53	130	64
MV	5		890	910	21	89	52

3.3 Performance of CO₂ sensors placed at the breathing height and on the desk

Above discussion suggests that in the room with displacement ventilation and high occupancy, it is necessary to find out a better sampling position for the measurement of the breathing zone CO₂ concentration. Therefore, the steady-state CO₂ concentrations at exhaust (Ex), at four sampling points placed at walls at 1.2 m height (S1-S4) and at two sampling points placed on the office desk (S5-S6) are measured and compared to the average concentration in the breathing zone.

Figure 10 shows the comparison results in the cases with five occupants. As shown in Figure 10a, with displacement ventilation and ACH of 2.5 h⁻¹, the CO₂ concentration at exhaust notably exceeds the tolerance level I, whereas all the concentrations at the sampling points S1-S4 lay in the tolerance level I and are fairly closer to the breathing zone concentration. Even the largest difference occurring at S4 is only 94 ppm, which is 50% of that occurring at exhaust (see Table

5), indicating a better performance of the sensor placed at wall at the 1.2 m height than that at exhaust. This phenomenon is caused by the stratification of the CO₂ concentration in the displacement ventilation system, while the concentration variation within the horizontal plane at the same height is not significant. Consequently, the sensors positioned within the height range of the breathing zone can more accurately represent the average concentration in it.

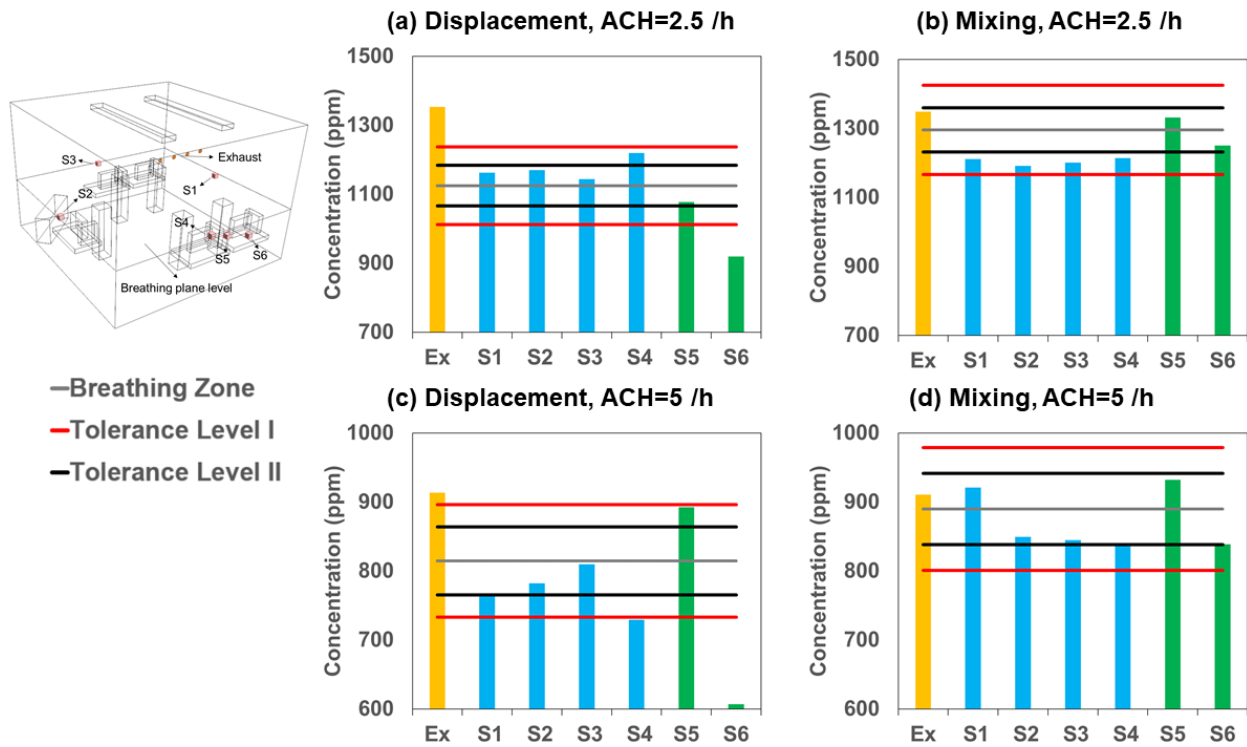


Figure 10. Comparisons between the steady-state CO₂ concentrations at exhaust (Ex) and at sampling points S1-S6 to the average CO₂ concentration in the breathing zone in the cases with five occupants.

For the sampling points on the office desk (S5-S6), the CO₂ concentration at S5 is within the tolerance level II, whereas the concentration at S6 is significantly lower than the breathing zone concentration. The difference between the measurements at these two sampling points is likely due to their different locations on the desk. S5 is placed beside the monitor while S6 is behind it and the monitor may block the access of CO₂ to S6 in this scenario.

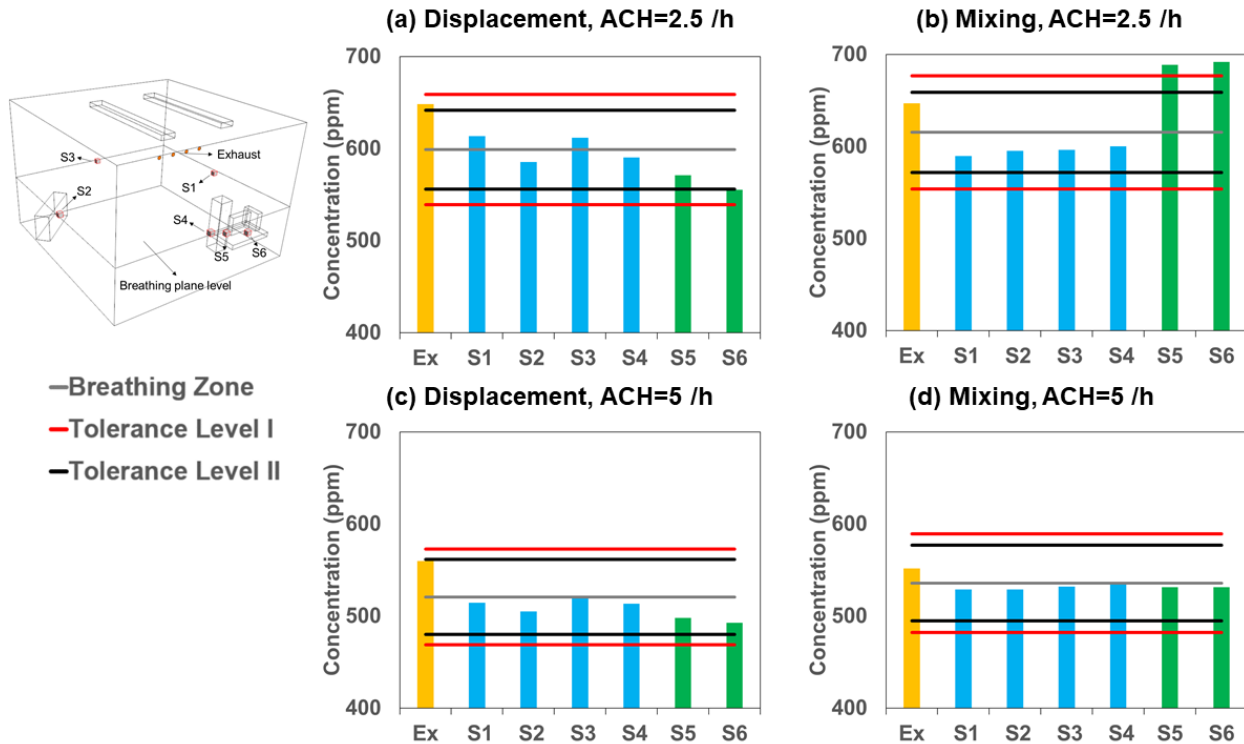


Figure 11. Comparisons between the steady-state CO₂ concentrations at exhaust (Ex) and at sampling points S1-S6 to the average CO₂ concentration in the breathing zone in the cases with one occupant.

The case with ACH of 5 h⁻¹ also demonstrates the similar results (see Figure 10c). However, with mixing ventilation, regardless of the ACH, all the CO₂ concentrations at exhaust as well as at S1-S6 are closer to each other and within the tolerance level I due to the homogeneous CO₂ distribution, as shown in Figure 10b and 10d. However, only the sensors at exhaust always read higher values and tend to result in the overventilation, while the outcomes from sensors at wall and desk are uncertain. Considering all the measured concentrations do not significantly differ from the breathing zone concentration, and overventilation is likely considered more acceptable than underventilation, the sensors placed at exhaust are recommended for the mixing ventilated room.

Figure 11 presents the comparison results in the cases with one occupant. Basically it demonstrates the similar trend with that for five occupants. The only difference is in the scenario with mixing ventilation and ACH of 2.5 h⁻¹ (see Figure 11b), the CO₂ concentrations at both S5 and S6 are noticeably larger than the breathing zone concentration and exceed the tolerance level I. These discrepancies are likely due to the insufficient air mixing around the occupant and computer when the ACH is relatively small. A large portion of CO₂ is trapped around the computer and causes much higher readings from the sensors on the desk. Table 5 summaries the steady-state CO₂ concentrations in the breathing zone, at the exhaust and at sampling points S1-S6.

Table 5. CO₂ concentrations at exhaust, in the breathing zone and at six sampling points (DV: displacement ventilation; MV: mixing ventilation; BZ: breathing zone)

Ventilation	ACH (h ⁻¹)	Occupant number	Steady-state CO ₂ concentration (ppm)							
			BZ	Ex	S1	S2	S3	S4	S5	S6
DV	2.5	1	599	648	614	585	612	590	571	555
DV	5		521	560	514	505	521	513	498	493
MV	2.5		615	647	590	595	596	600	689	692
MV	5		536	552	529	529	532	537	531	531
DV	2.5	5	1125	1353	1163	1170	1144	1219	1077	920
DV	5		814	913	764	782	810	729	892	607
MV	2.5		1296	1349	1211	1191	1200	1214	1331	1250
MV	5		890	910	921	850	845	836	932	839

These results suggest that in the displacement ventilated space, the CO₂ sensors situated at wall at the height of 1.2 m provide more accurate measurement of the breathing zone concentration than those at exhaust, while with mixing ventilation, it is recommended to place the sensors at exhaust. The performance of the sensors placed on the office desk vary notably under different conditions. This is likely because that the sensors are in the vicinity of CO₂ source (occupant) and several heat sources (monitor and computer). The CO₂ distribution pattern around them is

highly unstable and easily influenced by the change of building operating factors, causing the strong fluctuation of the sensor readings.

4. Conclusion

The present study examined the CO₂ dispersion pattern in occupied space under different conditions and tested the performance of the CO₂ sensors at various locations to evaluate the effect of the sensor position on the measurement for the demand controlled ventilation (DCV) system. Experimentally validated Computational Fluid Dynamics (CFD) models were employed to investigate the impacts of the ventilation strategy, air change rate (ACH) and the number of occupants. The following conclusions are obtained:

- 1) The ventilation strategy, air change rate and number of occupants have notable impacts on the CO₂ transport and sensor readings in the room. Displacement ventilation creates the concentration stratification and lower ACH causes a larger vertical gradient. The displacement ventilation with ACH of 2.5 hr⁻¹ yields a roughly 900 ppm vertical variation from the floor to the ceiling. Along the horizontal plane at the same height, the CO₂ distribution is nearly homogenous. With mixing ventilation, both the vertical and horizontal distributions are more uniform and the uniformity increases with larger ACH. This pattern is more noticeable when the occupancy increases.
- 2) The CO₂ sensors placed at exhaust only can accurately predict the breathing zone concentration in the mixing ventilated room and the discrepancies are within the uncertain of the CO₂ sensors used in experiments. With displacement ventilation, the sensors show less accuracy. For the room with low occupancy, due to less CO₂ emission, the discrepancies are smaller than 50 ppm and may be acceptable, while when the

occupant number increases to five, the sensor can cause a considerable discrepancy as 228 ppm.

- 3) In the displacement ventilation system, the CO₂ sensors situated at wall at the breathing height (e.g., 1.2 m) have better performance for the measurements of the breathing zone concentration than those at exhaust. In the room with 2.5 hr⁻¹ ACH and five occupants, the sensors at the breathing height can achieve at least 50% reduction of the difference between the sensor reading and the breathing zone concentration.
- 4) The performance of the CO₂ sensors placed on the office desk can vary significantly with ventilation strategy, air change rate and occupancy. The present study suggests a caution in using them for the DCV system. The reasonable analysis and careful prediction of the sensor performance should be conducted before using them.

Generally, the present study provides engineers and designers with the information for the CO₂ transport pattern in the typical office and the selection of the sensor position for the CO₂-based DCV system. The study results suggest in the mixing ventilated office, it is better to place the sensors at exhaust since they can accurately predict the breathing zone CO₂ concentration and only cause a little overventilation, which is better than underventilation may resulted from sensors at other sampling locations. However, when the office is equipped with displacement ventilation, the sensors can be positioned at wall at the breathing height (e.g., 1.2 m) since they can provide more accurate measurements than those at exhaust, especially with large occupancy. In addition, regardless of the ventilation strategy, the performance of the sensors placed on the office desk should be carefully tested before using them.

A few limitations should be noted. The present study was performed for a typical office, and the study results cannot be generalized for other types of the room with notably different geometries

and properties (e.g., the conference room and classroom). Also note that for all simulations, the exhaust is fixed at the ceiling level and the impact of the exhaust position is not reported. Future studies are warranted to investigate the CO₂ dispersion and measurement for the different types of the room, and the influence of the exhaust position should be considered.

REFERENCES

- Daisey, J. M., Angell, W. J., & Apte, M. G. (2003). Indoor air quality, ventilation and health symptoms in schools: an analysis of existing information. *Indoor air*, 13(1), 53-64.
- Sherman, M. H., & Matson, N. (1997). Residential ventilation and energy characteristics. *ASHRAE transactions*, 103(1), 717-730.
- Emmerich, S. J., & Persily, A. K. (1998). Energy impacts of infiltration and ventilation in US office buildings using multi-zone airflow simulation. *Proceedings of IAQ and Energy*, 98, 191-206.
- ASHRAE. (2013). ANSI/ASHRAE Standard 62.1-2013: Ventilation for Acceptable Indoor Air Quality. Atlanta, GA, USA: American Society of Heating, Refrigeration, and Airconditioning Engineers.
- Kusuda, T. (1976). Control of ventilation to conserve energy while maintaining acceptable indoor air quality. National Bureau of Standards, Department of Commerce.
- Nielsen, T. R., & Drivsholm, C. (2010). Energy efficient demand controlled ventilation in single family houses. *Energy and Buildings*, 42(11), 1995-1998.
- Budaiwi, I. M., & Al-Homoud, M. S. (2001). Effect of ventilation strategies on air contaminant concentrations and energy consumption in buildings. *International journal of energy research*, 25(12), 1073-1089.
- Faulkner, D., Fisk, W., & Walton, J. (1996). Energy savings in cleanrooms from demand-controlled filtration. *Journal of the IES*, 39(6), 21-27.
- Schibuola, L., Scarpa, M., & Tambani, C. (2016). Annual performance monitoring of a demand controlled ventilation system in a university library. *Energy Procedia*, 101, 313-320.
- Shan, K., Sun, Y., Wang, S., & Yan, C. (2012). Development and In-situ validation of a multi-zone demand-controlled ventilation strategy using a limited number of sensors. *Building and environment*, 57, 28-37.
- Fisk, W. J., & De Almeida, A. T. (1998). Sensor-based demand-controlled ventilation: a review. *Energy and buildings*, 29(1), 35-45.
- Krarti, M., & Al-Alaw, M. (2004). Analysis of the Impact of CO₂-Based Demand-Controlled Ventilation Strategies on Energy Consumption. *ASHRAE Transactions*, 110(1).
- Nassif, N., Kajl, S., & Sabourin, R. (2005). Ventilation control strategy using the supply CO₂ concentration setpoint. *Hvac&R Research*, 11(2), 239-262.
- Sun, Z., Wang, S., & Ma, Z. (2011). In-situ implementation and validation of a CO₂-based adaptive demand-controlled ventilation strategy in a multi-zone office building. *Building and Environment*, 46(1), 124-133.
- ASTM. (2012). D6245-12: Standard Guide for Using Indoor Carbon Dioxide Concentrations to Evaluate Indoor Air Quality and Ventilation. *American Society for Testing and Materials*.
- Persily, A. K. (1997). Evaluating building IAQ and ventilation with indoor carbon dioxide. *Transactions-American society of heating refrigerating and air conditioning engineers*, 103, 193-204.
- Lee, S. C., & Chang, M. (1999). Indoor air quality investigations at five classrooms. *Indoor air*, 9(2), 134-138.
- Stymne, H., Sandberg, M., & Mattsson, M. (1991, September). Dispersion pattern of contaminants in a displacement ventilated room-implications for demand control. In *Proceedings of the 12th AIVC Conference, Ottawa* (pp. 173-89).

- Mundt, E. (1994). Contamination distribution in displacement ventilation—influence of disturbances. *Building and environment*, 29(3), 311-317.
- Mahyuddin, N., & Awbi, H. (2010). The spatial distribution of carbon dioxide in an environmental test chamber. *Building and Environment*, 45(9), 1993-2001.
- Mahyuddin, N., & Awbi, H. (2012a). A review of CO₂ measurement procedures in ventilation research. *International Journal of Ventilation*, 10(4), 353-370.
- Bulińska, A., Popiołek, Z., & Buliński, Z. (2014). Experimentally validated CFD analysis on sampling region determination of average indoor carbon dioxide concentration in occupied space. *Building and Environment*, 72, 319-331.
- Mahyuddin, N., & Awbi, H. B. (2012b). MODELLING THE DISTRIBUTION OF EXHALED CO₂ IN AN ENVIRONMENTAL CHAMBER. In *10th International conference, healthy buildings 2012*.
- Rim, D., Novoselac, A. (2008). Transient simulation of airflow and pollutant dispersion under mixing flow and buoyancy driven flow regimes in residential buildings. *Ashrae Transactions*, 114, 130.
- Ning, M., Mengjie, S., Mingyin, C., Dongmei, P., & Shiming, D. (2016). Computational fluid dynamics (CFD) modelling of air flow field, mean age of air and CO₂ distributions inside a bedroom with different heights of conditioned air supply outlet. *Applied energy*, 164, 906-915.
- Zhuang, R., Li, X., & Tu, J. (2014, June). CFD study of the effects of furniture layout on indoor air quality under typical office ventilation schemes. In *Building Simulation* (Vol. 7, No. 3, pp. 263-275). Springer Berlin Heidelberg.
- Chen, Q., & Srebric, J. (2002). A procedure for verification, validation, and reporting of indoor environment CFD analyses. *HVAC&R Research*, 8(2), 201-216.
- Persily, A., & Jonge, L. (2017). Carbon dioxide generation rates for building occupants. *Indoor air*, 27(5), 868-879.
- Topp, C., Nielsen, P. V., & Sorensen, D. (2002). Application of computer simulated persons in indoor environmental modeling/discussion. *ASHRAE transactions*, 108, 1084.
- Deevy, M., & Gobeau, N. (2006). CFD modelling of benchmark test cases for a flow around a computer simulated person. HSL/2006/51.
- Peric, M., & Ferguson, S. (2012). The advantage of polyhedral meshes. *Dynamics*, 24, 45.
- CD-adapco. (2012) USER GUIDE: STAR-CCM+. Version 12.02.011.
- Menter, F. R. (1994). Two-equation eddy-viscosity turbulence models for engineering applications. *AIAA journal*, 32(8), 1598-1605.
- Argyropoulos, C. D., & Markatos, N. C. (2015). Recent advances on the numerical modelling of turbulent flows. *Applied Mathematical Modelling*, 39(2), 693-732.
- Gilani, S., Montazeri, H., & Blocken, B. (2016). CFD simulation of stratified indoor environment in displacement ventilation: Validation and sensitivity analysis. *Building and Environment*, 95, 299-313.
- ASHRAE. (2013). *ASHRAE Handbook—Fundamentals*. Atlanta, GA, USA: American Society of Heating, Refrigeration, and Airconditioning Engineers.
- Mundt, E. (1990). Convection flows above common heat sources in rooms with displacement ventilation. In *Proceedings of ROOMVENT*, Vol. 90, pp. 13-15.
- Rim, D., & Novoselac, A. (2009). Transport of particulate and gaseous pollutants in the vicinity of a human body. *Building and Environment*, 44(9), 1840-1849.
- Maldonado, E. A. B., & Woods, J. E. (1983). A method to select locations for indoor air quality sampling. *Building and Environment*, 18(4), 171-180.

ASTM. (2011). E741-11. Standard test method for determining air change in a single zone by means of a tracer gas dilution. *American Society for Testing and Materials*.